Hindawi
Journal of Chemistry
Volume 2022, Article ID 8260379, 14 pages
https://doi.org/10.1155/2022/8260379

Research Article

Extraction and Identification of Antioxidant Ingredients from *Cyclocarya paliurus* (Batal.) Iljinsk Using UHPLC-Q-Orbitrap-MS/MS-Based Molecular Networking

Yingpeng Tong,[1,2] **Xin Li**,[2] **Ziping Zhu**,[2] **Ting Wang**,[1] **Qi Zhou**,[1] **Na Li**,[2] **Zhenda Xie**,[1] **Chunxiao Jiang**,[1] **Junmin Li**,[1,2] **and Jianxin Wang**[1,3,4]

[1]*School of Advanced Study, Taizhou University, Taizhou 318000, China*
[2]*Zhejiang Provincial Key Laboratory of Evolutionary Ecology and Conservation, Taizhou University, Taizhou 318000, China*
[3]*Department of Pharmaceutics, School of Pharmacy, Fudan University & Key Laboratory of Smart Drug Delivery, Ministry of Education, Shanghai 201203, China*
[4]*Institute of Integrative Medicine, Fudan University, Shanghai 201203, China*

Correspondence should be addressed to Junmin Li; lijmtzc@126.com and Jianxin Wang; jxwang@fudan.edu.cn

Received 25 August 2022; Revised 9 November 2022; Accepted 9 December 2022; Published 26 December 2022

Academic Editor: Beatriz P. P. Oliveira

Cyclocarya paliurus (Batal.) Iljinskaja (LCP) leaves have been widely employed in food and traditional medicine for treating hyperlipidaemia and its complications, possibly owing to their antioxidant properties. The aim of the present study is to identify the chemical ingredients of antioxidant extracts from LCP by using UHPLC-Q-Orbitrap-MS/MS-based molecular networking, a very recent and useful tool for annotation of chemical constituents in mixtures. The extraction conditions of antioxidant extracts from LCP were optimised by single-factor analysis and response surface methodology (RSM). The optimised conditions were a methanol concentration of 32%, a liquid-to-solid ratio of 0.4 ml/mg, an extraction temperature of 25°C, and an extraction time of 32 min. Under these conditions, the antioxidant yield was 516.20 ± 28.52 μmol TE/ml. The main active ingredients in the antioxidants were identified by UHPLC-Q-Exactive Orbitrap-MS-based molecular networking. In total, 42 compounds were identified, including 20 flavonoids, 16 quinic acid derivatives, 4 caffeoyl derivatives, and 2 coumaroyl derivatives. The findings of the present work suggest that LCP could be a suitable source of natural antioxidant compounds, which might be applicable in the development of potential pharmaceutical drugs targeting diseases related to oxidative stress.

1. Introduction

Cyclocarya paliurus (Batal.) Iljinskaja (LCP), the sole species in the genus *Cyclocarya Iljinskaja*, is widely distributed in the mountainous regions at heights of 420–2500 m [1]. LCP has a very sweet taste and is used as "sweet tea" in traditional medicine in China [2]. LCP was approved for use as a new edible raw material by the National Health and Family Planning Commission of China; consequently, since 2013, the demand for LCP, an important and valuable crop, has been increasing [3]. To our best knowledge, at least three functional foods containing LCP have been approved for sale in China; these are consumed to lose weight and regulate blood sugar, blood lipids, and high blood pressure. These products are believed to be very beneficial for the prevention and regulation of hyperlipidaemia [4], nonalcoholic fatty liver disease (NAFLD) [5], and diabetes [6]. Oxidative stress is considered a common underlying cause for these diseases [7–9], and numerous studies have proved that antioxidant ingredients are effective against them [10–13]. Therefore, considering their potential health benefits, it is important to identify the components contributing to the antioxidant activity of LCP.

To date, more than 200 compounds have been isolated from LCP, including flavonoids, phenolic acids, polysaccharides, and triterpenoids. Some have been proven to

possess significant antioxidant activities. Crude polysaccharides from LCP, extracted by an ultrasonic-assisted method, could be used to scavenge 92.09% of 1,1-diphenyl-2-picrylhydrazyl 2,2-diphenyl-1-(2,4,6-trinitrophenyl) hydrazyl (DPPH) free radicals at 0.25 mg/ml [14]. A water-soluble polysaccharide was further isolated by column chromatography and was reported to provide anti-DPPH radical activity with an EC_{50} value of 52.3 μg/ml [15]. In addition, there is a significant geographic relation with water-soluble polysaccharide content and scavenging activities of LCP [16]. Flavonoids are believed to possess strong antioxidant activity [17]. The antioxidant activities of flavonoids extracted from LCP have been studied, with the IC_{50} value for the DPPH radical-scavenging ability ranging from 0.025 mg/ml to 0.146 mg/ml [1, 18, 19]. In addition, phenolic acids, such as chlorogenic acid, are also considered to possess strong antioxidant activity [20]. In addition to the different origins of raw materials, the different extraction methods and their extraction conditions might be the main reasons for the differences in the antioxidant activity of the extracts. However, thus far, a preparation process for the antioxidant extracts from LCP has not yet been established and optimised. Furthermore, few reports have focused on identifying the chemical components in LCP antioxidant extracts.

There exist various mass spectrometric platforms for the identification and quantification of chemical constituents in Traditional Chinese Medicine (TCM), such as quadrupole-time of flight (Q-TOF) [21], Fourier-transform ion cyclotron resonance (FTICR) [22], and Orbitrap [23]. Among them, Orbitrap is the newest member of the high-resolution mass spectrometric (HRMS) analysers. Combined with ultrahigh-performance liquid chromatography (UHPLC), it is a useful tool for the identification of chemical ingredients in TCM by providing the exact mass and a possible chemical formula of the ingredients. However, it is very time-consuming to extract effective chemical structure information from the large amounts of data generated by the analysis of complex mixtures by UHPLC-HRMS. MS/MS-based molecular networking (MN) is a very recent and useful method for metabolite annotation and has attracted significant interest in TCM research [24–28]. To our knowledge, there is no report on the identification of the antioxidant ingredients in LCP using this method.

In the present study, to systematically investigate the ultrasonic-assisted extraction (UAE) process and chemical composition of the antioxidant extracts of LCP, single-factor experiments were first conducted to screen the key factors and their suitable ranges of multiple extraction variables. Subsequently, a three-level, three-variableBox-Behnken design (BBD) was sequentially employed to optimise the UAE conditions. Finally, UHPLC-Q-Orbitrap-MS/MS-based MN was performed to identify the antioxidant ingredients in LCP. This research may provide a scientific basis for the development, utilization, and quality control of the antioxidant extracts of LCP.

2. Materials and Methods

2.1. Chemicals and Plant Materials. Six reference compounds with a purity higher than 98% (w/w), including chlorogenic acid, myricitrin, quercitrin, isoquercitrin, hyperoside, and afzelin, were purchased from Chengdu Alfa Biotechnology Co., Ltd. Substances used to evaluate the antioxidant activity, including DPPH, 2,4,6-tripyridyl-s-triazine (TPTZ), and 2,2′-azino-bis (3-ethylbenzothiazoline-6-sulfonic acid) (ABTS), were obtained from Yuanye Biological Technology Co., Ltd. HPLC-grade acetonitrile and methanol were obtained from Tedia Company. All the other chemicals were reagent grade.

Approximately 10 kg of dried leaves of LCP were picked in Suichang, Zhejiang Province, China, in May 2019 and identified by Professor Junmin Li. They were maintained in a 4°C refrigerator until the subsequent experiments.

2.2. Antioxidant Activity Assays. Based on methods reported previously with minor modifications, a ferric-reducing antioxidant power (FRAP) assay, ABTS•+, and DPPH radical scavenging assays were applied to evaluate the antioxidant activity of the LCP extracts, which is expressed as μmol Trolox (TE)/dry sample (g) (μmol TE/g) [29–31].

2.3. Ultrasound-Assisted Extraction of Antioxidants in LCP

2.3.1. Extraction Process and Single-Factor Experiment Design. UAE was performed to extract antioxidants from LCP using a DL-720J ultrasonic extractor (Shanghai Zhixin Instrument Co., Ltd.). Firstly, about 0.5 g LCP powder was accurately weighted and extracted under the following conditions: extraction solvents, water, 25%, 50%, 75%, or 100% methanol aqueous solution; different sample-to-solvent ratios (0.1, 0.2, 0.3, 0.4, and 0.5 mg/ml); different temperatures (25, 35, 45, and 55°C); and different times (15, 30, 45, 60, and 75 min). The extraction solution was centrifuged at 3500 rpm for 15 min after cooling to room temperature. Subsequently, the antioxidant capacities (μmol TE/g) of the suspensions were evaluated by the DPPH radical-scavenging assay.

2.3.2. BBD Optimisation. The UAE conditions were further optimised by the BBD with response surface methodology (RSM) in Design Expert Version 10.0.7 software (Stat-Ease, Inc., USA). Based on the results of single-factor experiments, the methanol concentration (X1), extraction time (X2), and liquid-to-solid ratio (X3) were selected as the independent variables, each with three levels (Table 1). The antioxidant capacity (μmol TE/g) of the extraction solution was set as a responding value (Y).

2.4. UHPLC-Q-Orbitrap-MS/MS Conditions. The chromatographic separation of chemical ingredients from the antioxidant extraction solution of LCP was completed on the Ultimate R3000 UHPLC apparatus (Thermo Fisher Scientific, Waltham, MA, USA) with ACQUITY UHPLC HSS T3 (2.1 × 100 mm, 1.8 μm, Waters Corporation, Milford, CT, USA). A mobile phase containing acetonitrile (eluent A) and water with 0.5% formic acid (eluent B) was used in the following solvent gradient system: 0–6 min, 10% A;

Table 1: Comprehensive evaluation for the extracts in single-factor experiments.

Independent variables	Levels		
	−1	0	1
Methanol concentration (%, X1)	0	25	50
Extraction time (min, X2)	15	30	45
Liquid-solid ratio (ml/mg, X3)	0.3	0.4	0.5

6–15 min, 10–13.5% A; 15–21 min, 13.5–21% A; 21–30 min, 21–25% A; 30–60 min, and 25–100% A. The flow rate, column temperature, and injection volume were set at 0.2 ml/min, 35°C, and 10 μl, respectively.

A Q-Exactive™ mass spectrometer (Thermo Scientific, Sunnyvale, CA, USA), equipped with a heated ESI (HESI-II; Thermo Scientific), was employed for the MS analysis. The ESI was operated under the following parameters: heater temperature, 300°C; capillary temperature, 325°C; electrospray voltage, 3.2 kV; sheath gas flow rate, 30 l/min; auxiliary gas flow rate, 10 l/min; sweep gas flow rate, 2 l/min. High-resolution mass spectra were acquired in the positive and negative modes separately. The acquisition modes of the quadrupole-Orbitrap analyses were set to be the full MS/dd-MS^2 (TopN) mode and full MS mode. The full MS mode was employed with an applied mass scan range of 100–1500 m/z, an Orbitrap resolution of 70,000 a maximum ion injection time (IT) of 200 ms, and an automatic gain control (AGC) target value of 3×10^6. The dd-MS^2 mode was operated in the TOP5 mode, using the following settings: an Orbitrap resolution of 17,500 with the maximum IT of 50 ms and an AGC target value of 3×10^6, a loop count of 5, an isolation window of 4, and stepped normalised collision energy (NCE) values of 20, 40, and 60.

2.5. Data Preprocessing and Statistical Analysis. Xcalibur software (Thermo Fisher Scientific, USA) was used to extract information on the retention time (RT), accurate molecular weight (m/z), and MS/MS fragment ions from the raw data obtained by UHPLC-Orbitrap-MS/MS analysis. The raw MS/MS data were converted to the mzXML format and further processed by MZmine 2.5.3. These data were uploaded to the GNPS platform (https://gnps.ucsd.edu), and a molecular network was generated following the workflow of feature-based molecular networking (FBMN) [32]. The networking parameters were as follows: mass tolerance of 0.0075 Da, matched peaks greater than 6, and a cosine score greater than 0.7. MolNetEnhancer, another tool in GNPS, was used to annotate the chemical classes of the nodes in the molecular network [33]. Simultaneously, an in-house compound database for LCP, which included the compound name, molecular formula, and calculated mass ($[M-H]^-$/$[M+H]^+$), was established by searching online databases, including the Chinese National Knowledge Infrastructure and Web of Science databases. This developed database can provide reference information for annotating the chemical structure of the nodes in the molecular network.

3. Results and Discussion

3.1. Screening Experimental Factors of Extraction Processes

3.1.1. Influence of Methanol Concentration. For an extraction temperature, extraction time, and liquid-solid ratio of 25°C, 30 min, and 0.3 ml/mg, respectively, the influence of different methanol concentrations on the antioxidant yield was compared, and the results are shown in Figure 1(a). When the extraction solvent was 25%, 50%, or 75% methanol, the antioxidant yields were significantly higher than that when the extraction solvent was water or anhydrous methanol. Moreover, the antioxidant yield for extraction with water was also significantly higher than that for extraction with anhydrous methanol. This result may be attributed to the higher water solubility of the active ingredients in the antioxidants from LCP, such as polysaccharides [34] and flavonoid glycosides [19]. Considering that the highest antioxidant yield was obtained via extraction with 25% methanol, this solvent was chosen as the extraction solvent for subsequent analyses.

3.1.2. Influence of Extraction Temperature. When determining the influence of the extraction temperature (25, 35, 45, and 55°C) on antioxidant yields, the methanol concentration, extraction time, and liquid-solid ratio were set at 25%, 30 min, and 0.3 ml/mg, respectively. As shown in Figure 1(b), the antioxidant yield was highest when the extraction temperature was set at 25°C; it significantly decreased with increasing extraction temperature thereafter, which might be related to the degradation of phenolic compounds. Phenolic compounds typically exhibit good antioxidant activity [35], but may be degraded by prolonged ultrasonic treatment at higher temperatures. As reported by Ma [36], after ultrasonic treatment at 40°C for 20 min, the contents of caffeic acid, *p*-coumaric acid, ferulic acid, and *p*-hydroxybenzoic acid decreased by 48.90%, 44.20%, 48.23%, and 35.33%, respectively. In the present work, the influence of a temperature lower than 25°C on the antioxidant yield was not studied because the room temperature in this experiment was ~25°C; to lower the experimental temperature, the experimental steps would have to be increased, which would affect the accuracy of the experimental results. Hence, the optimum extraction temperature was selected as 25°C.

3.1.3. Influence of Extraction Time. When determining the effects of extraction time (15, 30, 45, 60, and 75 min) on the antioxidant yield, the methanol concentration, extraction temperature, and liquid-solid ratio were set at 25%, 25°C, and 0.3 ml/mg, respectively. As shown in Figure 1(c), for an extraction time in the range of 15–30 min, the antioxidant yield was notably enhanced ($P < 0.05$). As the extraction time increased from 30 to 45 min, it had a notable decreasing effect on the antioxidant yield ($P < 0.05$). When the extraction time was increased from 45 to 75 min, the antioxidant yield slightly increased, but there was no significant difference among the results. The above experimental results indicated that prolonged extraction could decrease the

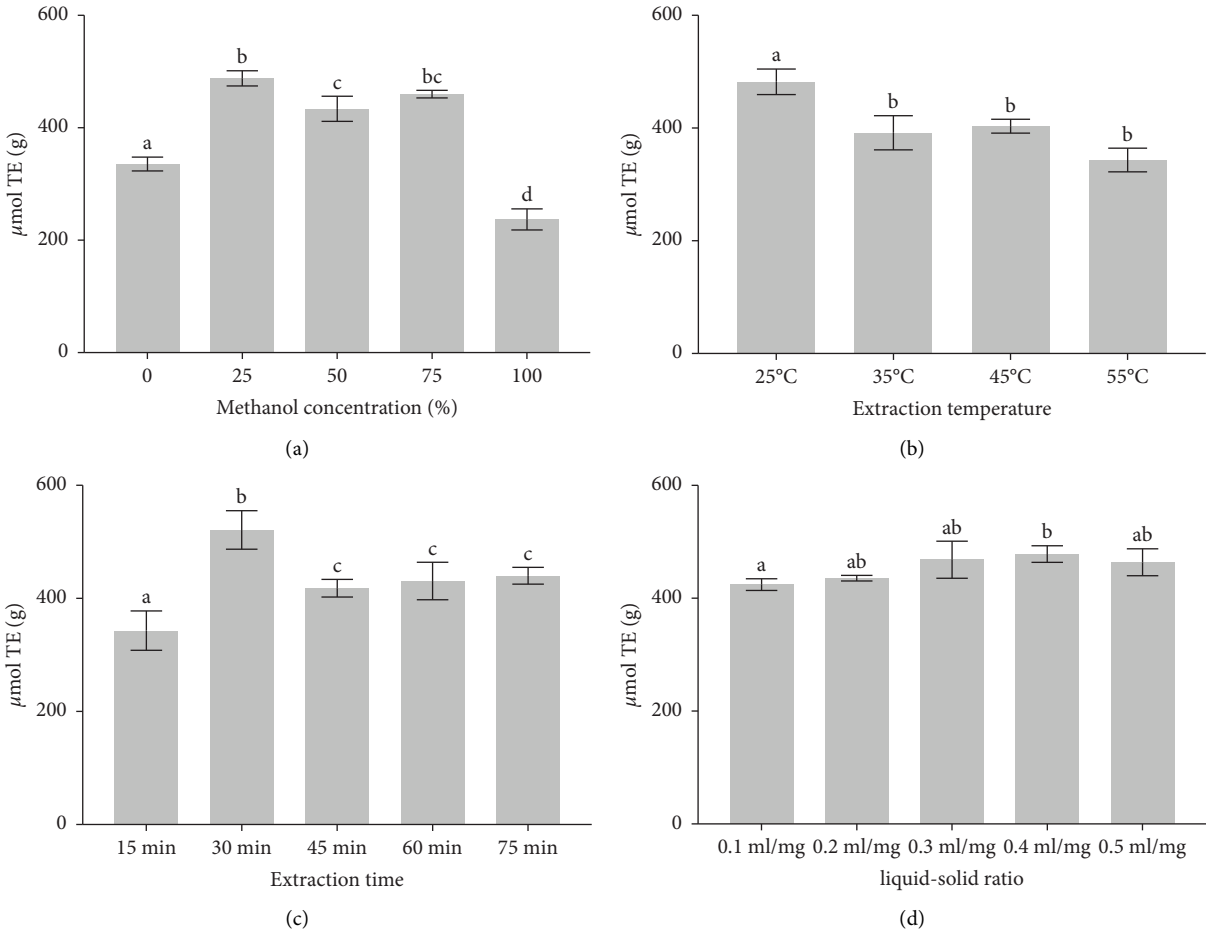

Figure 1: Influence of methanol concentration (a), extraction temperature (b), extraction time (c), and liquid-solid ratio (d) on the yields of antioxidants from LCP.

antioxidant yield due to the instability of the main antioxidant ingredients, such as phenolic compounds [37]. Therefore, the extraction time was set at 30 min.

3.1.4. Influence of Liquid-Solid Ratio. The methanol concentration, extraction temperature, and extraction time were set at 25%, 25°C, and 30 min, respectively, to determine the effects of the liquid-solid ratio (0.1, 0.2, 0.3, 0.4, and 0.5 ml/mg) on the antioxidant yields. Figure 1(d) shows that the antioxidant yield from LCP gradually increases when the liquid-solid ratio increases from 0.1 to 0.4 ml/mg. However, when the liquid-solid ratio is greater than 0.4 mg/ml, the antioxidant yield does not increase further. Therefore, the liquid-solid ratio was set at 0.4 ml/mg.

3.2. Optimisation of UAE Condition

3.2.1. Prediction Model and ANOVA. Considering that an extraction temperature higher than room temperature (~25°C) negatively affected the antioxidant yield and was also inconvenient for the extraction process, the extraction temperature was fixed at 25°C for subsequent extraction process optimisations in our work. Following the BBD, 17 trials were conducted to optimise the methanol concentration, extraction time, and liquid-solid ratio, which are listed in Table 2. The influence of the three extraction variables on the antioxidant yields was calculated to achieve the best fit equation, which is expressed as follows:

$$Y = 508.14 + 44.22 \times X1 + 12.40 \times X2 - 4.61 \times X3 - 1.57 \times X1 \times X2 - 4.38 \times X1 \times X3 + 1.62 \times X2 \times X3 - 74.22 \times X1\text{^}2 - 49.75 \times X2\text{^}2 - 42.62 \times X3\text{^}2. \quad (1)$$

As listed in Table 3, the obtained regression relation between the antioxidant yield and the three variables was significant ($P < 0.0001$) with a high degree of correlation ($R^2 = 0.9834$). The regression model also exhibited good reliability because the P value for a lack of fit was higher than 0.05. Moreover, the calculated data may not show a significant difference with the experimental data because of the low coefficient of variation (CV = 2.87%). The A_{deq} precision value was 19.623, which indicated that the signal was adequate without high levels of noise [38]. The P values of X1 and X2 were lower than 0.05, indicating that the methanol concentration and extraction time notably influenced the

Table 2: Box–Behnken design and response data for antioxidants yields.

Run	X1	X2	X3	Extraction yield (μmol TE/g)
1	−1	1	0	347.63
2	1	0	1	427.28
3	1	−1	0	423.84
4	0	1	−1	438.19
5	0	1	1	435.92
6	0	−1	−1	398.86
7	−1	−1	0	337.48
8	0	0	0	510.33
9	0	0	0	510.99
10	0	−1	1	390.11
11	0	0	0	491.7
12	−1	0	−1	346.54
13	1	0	−1	448.97
14	0	0	0	514.84
15	0	0	0	512.85
16	−1	0	1	342.38
17	1	1	0	427.73

Table 3: ANOVA for the response surface quadratic model of antioxidants yield.

Source	Sum of squares	*df*	Mean square	*F* value	*P* value
Model	62876.9	9	6986.32	45.96	<0.0001
X1	15645.92	1	15645.92	102.92	<0.0001
X2	1229.58	1	1229.58	8.09	0.0249
X3	169.92	1	169.92	1.12	0.3255
X1X2	9.8	1	9.8	0.0644	0.8069
X1X3	76.83	1	76.83	0.5054	0.5001
X2X3	10.5	1	10.5	0.0691	0.8003
X12	23197.11	1	23197.11	152.6	<0.0001
X22	10420.16	1	10420.16	68.55	<0.0001
X32	7649.98	1	7649.98	50.32	0.0002
Residual	1064.1	7	152.01		
Lack of fit	713.84	3	237.95	2.72	0.1793
Pure error	350.27	4	87.57		
Cor total	63941	16			
Adeq precision	19.263				

antioxidant yield, which is consistent with the results of the single-factor experiment.

3.2.2. Response Surface Plot and Contour Plot. The obtained regression model between the antioxidant yield and the three variables is also depicted in the form of a response surface plot and its corresponding contour plot (Figure 2). The contour plots were elliptical, as shown in Figures 2(b), 2(d), and 2(f), suggesting that the mutual interactions among the variables were not notable, consistent with the ANOVA result in Table 3.

3.2.3. Optimisation of the Regression Model. By setting the extraction yield to the maximum, the three independent variables, i.e., the liquid-solid ratio, methanol concentration, and extraction time, were optimised to 0.4 ml/mg, 32% methanol, and 32 min, respectively. With these optimised extraction conditions, the predicted antioxidant yield from LCP was 515.637 μmol TE/g. A verification test was then conducted, and the antioxidant yields achieved were 516.20 ± 28.52 μmol TE/g ($n = 6$); thus, there was no notable difference with the predicted value. Therefore, it is feasible to use this regression model to predict the yield of antioxidant extracts from LCP. The antioxidant capacities of the extraction solutions were also measured using the ABTS and FRAP assays. They are presented as Trolox equivalent values, which were 1027.36 ± 77.68 and 480.92 ± 32.77 μmol TE/g, respectively. Thus, LCP offers better antioxidant activity than some commonly used herbal teas, such as loquat leaf tea, which also has hypoglycaemic activity [39].

3.3. MS/MS-Based MN of Compounds in Antioxidant Extracts of LCP. The total ion chromatograms (TICs) of the LCP antioxidant extraction solution in the negative ion mode are shown in Figure 3. In the present work, a molecular network with 1290 precursor ions was generated. MN is a useful computing strategy based on MS/MS profiles. It can cluster compounds displaying similar fragment ions into the same group. The MN of the compounds in the antioxidant extracts

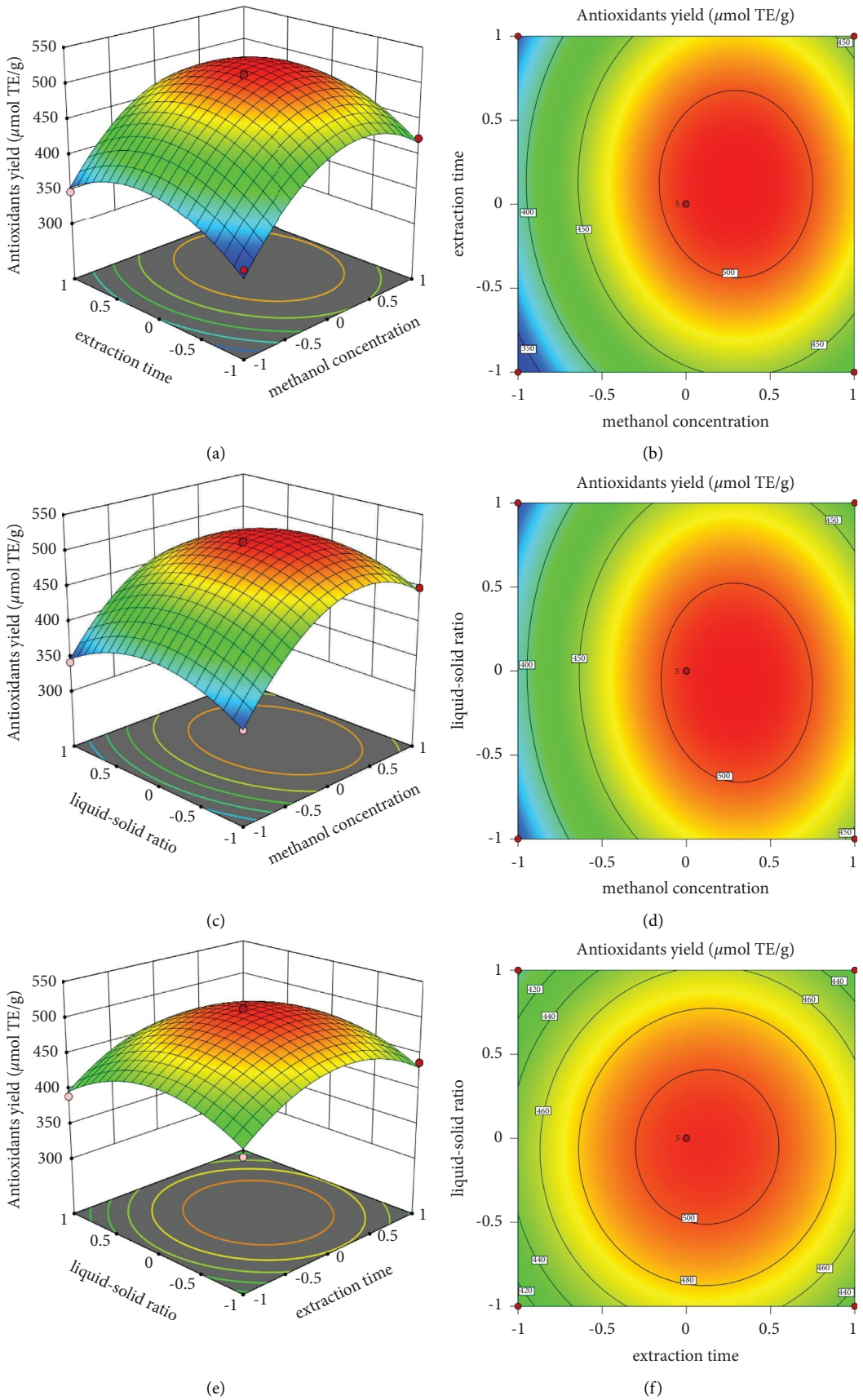

Figure 2: Response surface showing the effect of methanol concentration, extraction time, and liquid-solid ratio on the response Y (antioxidants yield).

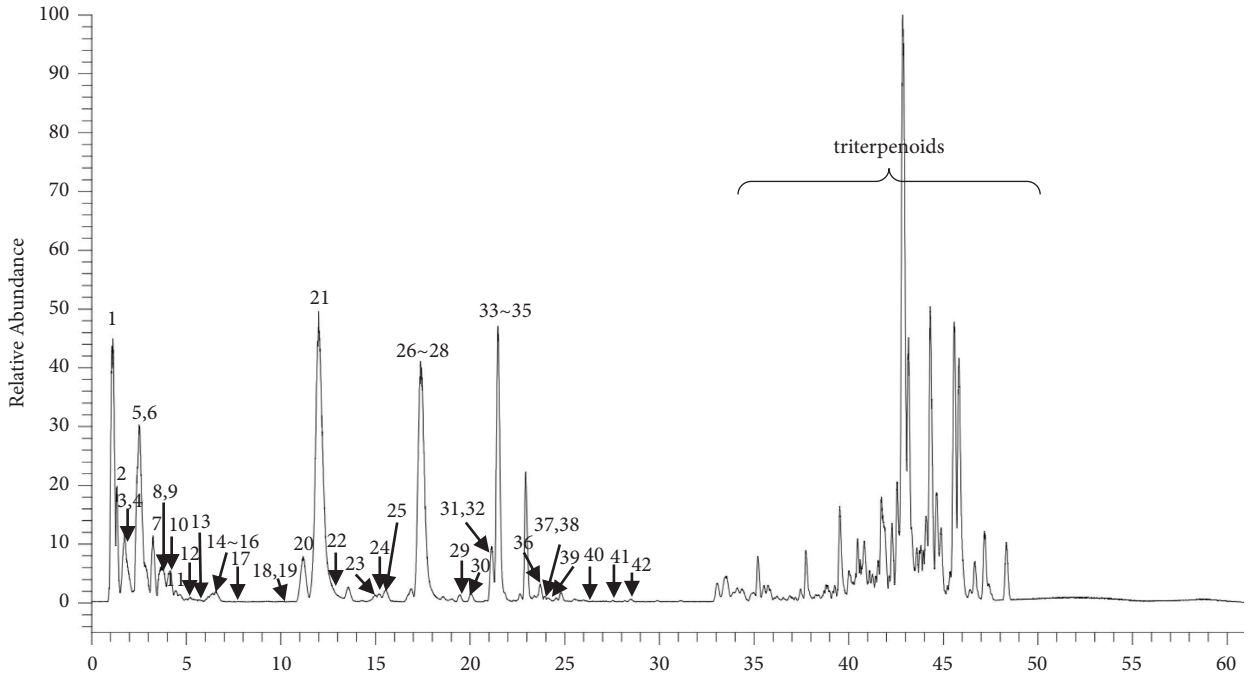

Figure 3: The total ion chromatograms of the LCP extraction solution in negative ion mode.

of LCP results in 101 clusters (nodes ≥2) and 597 single nodes, as shown in Figure 4. The results can be downloaded from the following link: https://gnps.ucsd.edu/ProteoSAFe/status.jsp?task=c6873f9e7f9a4da7aeb6230d2ac03cff. Based on the analysis results of MolNetEnhancer, the structures of nodes in the molecular network were annotated at the class level, and the results are available at the following link: https://gnps.ucsd.edu/ProteoSAFe/status.jsp?task=3f544c52f2e5454181ee85f45c964b7b. The structure classes are marked in different colours in Figure 4. The structure class of part nodes with grey colour was annotated not by MolNetEnhancer but by an in-house database together with their MS^2 spectra. They were marked with a dashed box and directly annotated in Figure 4. The classes include flavonoids, quinic acids and derivatives, hydroxybenzoic acid derivatives, O-glycosyl compounds, and fatty acids.

According to the molecular weights and characteristic fragments in the developed database of compounds from LCP, the nodes of triterpenoids were also screened via MN and are shown in Figure 4. Numerous studies have proved that flavonoids and phenolics have stronger antioxidant activity than triterpenoids [40]; therefore, in the present work, we mainly focused on the former classes in antioxidant extraction from LCP by comparison with the reference standards, in-house compound database, and GNPS library. In all, 42 compounds in LCP with an antioxidant activity were definitively or tentatively characterised, including 20 flavonoids, 16 quinic acid derivatives, 4 caffeoyl derivatives, and 2 coumaroyl derivatives. Detailed information, including the RT, MS/MS fragment ions, compound names, and structure types, is provided in Table S1.

3.3.1. Identification of Flavonoids. Flavonoids are among the most important active ingredients of LCP, possessing significant antioxidant activity [41]. The chemical class of compounds in molecular networking was annotated by MolNetEnhancer at different levels, including CF_superclass, CF_class, CF_subclass, and CF_department. In the level of CF_class, the chemical class of nodes in Figure 5 was all annotated as flavonoids, while they were divided into different classes in the level of CF_department, including flavonoid-3-O-glycosides, flavonoid-7-O-glycosides. Therefore, clusters CF1-CF4 mainly comprise nodes of flavonoids in separate form. In all, 26 nodes were annotated according to the literature and the GNPS database. These nodes represented the $[M-H]^-$, $[2M\text{-}H]^-$, $[M + FA\text{-}H]^-$, and/or $[3M\text{-}H]^-$ ions of 20 flavonoids from LCP (Table S1). Except kaempferol (no. 42) and quercetin (no. 36), which were included in Clusters F2 and CF4, the other 19 flavonoids were flavonoid glycosides. Among these 19 flavonoid glycosides, the signals at m/z 285, 317, and 301 in the MS^2 spectra correspond to kaempferol, myricetin, and quercetin, which are the most common aglycones of flavonoids in LCP. Additionally, neutral losses of 190 Da (glucuronyl), 162 Da (glucosyl or galactosyl), 146 Da (rhamnosyl), and 132 Da (arapyranosyl) could be observed in the MS^2 spectra of flavonoid glycosides. By comparing with reference standards, five compounds were explicitly identified as being myricitrin (no. 18), isoquercitrin (No. 20), hyperoside (no. 22), quercitrin (no. 27), and afzelin (No. 33), which are all flavonoid-3-O-glycosides and are present in Cluster CF1. A comparison of the relative abundances of the $[Aglycone\text{-}H]^-$ and $[Aglycone\text{-}H]^{-\bullet}$ ions is an effective method to determine the glycosylation position of flavonoids [42]. For

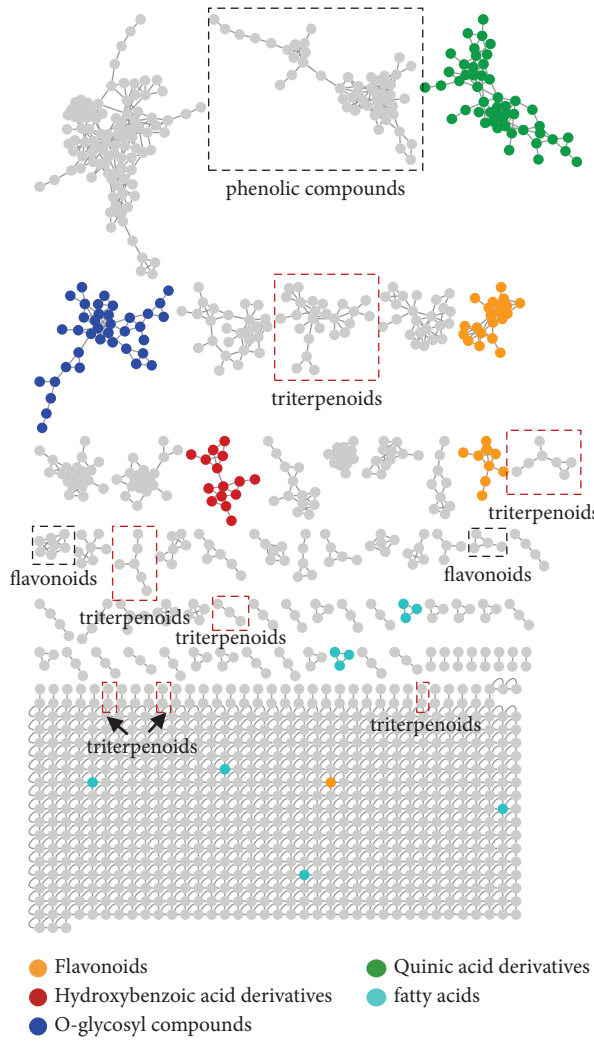

FIGURE 4: The global molecular networking of antioxidant extracts of LCP. The chemical classes of nodes, filled with different colours except for grey, were annotated by MolNetEnhancer. The structure classes of part nodes marked with grey and with a dashed box were annotated by an in-house database together with their MS^2 spectra. The structure classes of rest nodes with grey colour are not annotated in present work.

example, for isoquercitrin displayed in Figure 5(a), the relative abundance of the $[Aglycone\text{-}H]^{-\bullet}$ ions (m/z 300.02) in the MS^2 spectra is remarkably higher than that of the $[Aglycone\text{-}H]^-$ ions (301.03), indicating that the sugar unit was linked to the 3-O-position of flavonoids [43]. Similarly, the relative abundances of the $[Aglycone\text{-}H]^{-\bullet}$ ions of other compounds in Cluster CF1 are all higher than those of the $[Aglycone\text{-}H]^-$ ions, suggesting that the sugar moieties of these compounds were all linked to the 3-O-position. Similar to compound 21 in Figure 5(b), the relative abundances of the $[Aglycone\text{-}H]^{-\bullet}$ ions are remarkably lower than those of the $[Aglycone\text{-}H]^-$ ions in the MS^2 spectra of compounds from CF2 and CF3; the compounds of these clusters are significantly different from those in Cluster CF1, indicating that the sugar moieties in these two clusters were linked to the 7-O-position.

Compound 13 showed $[M\text{–}H]^-$ ions at m/z 593.1521 ($C_{27}H_{30}O_{15}$) and neutral losses of 146 and 132 Da in the MS^2 spectra in Figure 5(c), producing fragment ions at m/z 284.0298 (14.11), 285.0408 (100), and 447.0919 (7.9); this indicates that compound 13 was a kaempferol derivative containing hexose and deoxyhexose units. Because of the presence of $[M\text{-}Rha]^-$ (m/z 447.0919) and the higher relative abundance of $[Aglycone\text{-}H]^-$ ions at m/z 285.0408, two sugar units of compound 13 might be attached to the 7-O-position of kaempferol by forming a disaccharide. Thus, compound 13 was tentatively identified as kaempferol-7-O-glucoside-O-rhamnoside.

3.3.2. Identification of Phenolic Compounds. In addition to flavonoids, other types of phenolic compounds were also separated from LCP, such as caffeoyl quinic acids, which also possess strong antioxidant activities [44, 45]. In plants, quinic acid is naturally esterified with a large group of hydroxycinnamic acids, the majority of which are *p*-coumaric acid, caffeic acid, ferulic acid, and sinapic acid [46]. In this work, quinic acid derivatives, with characteristic fragment ions at m/z 191.06 ($[quinic\ acid\text{-}H]^-$), m/z 173.0455 ($[quinic\ acid\text{-}H\text{-}H_2O]^-$), and/or m/z 127.04 ($[quinic\ acid\text{-}H\text{-}H_2O\text{-}HCOOH]^-$), are present in the cluster as shown in Figure 6(a) according to the results of

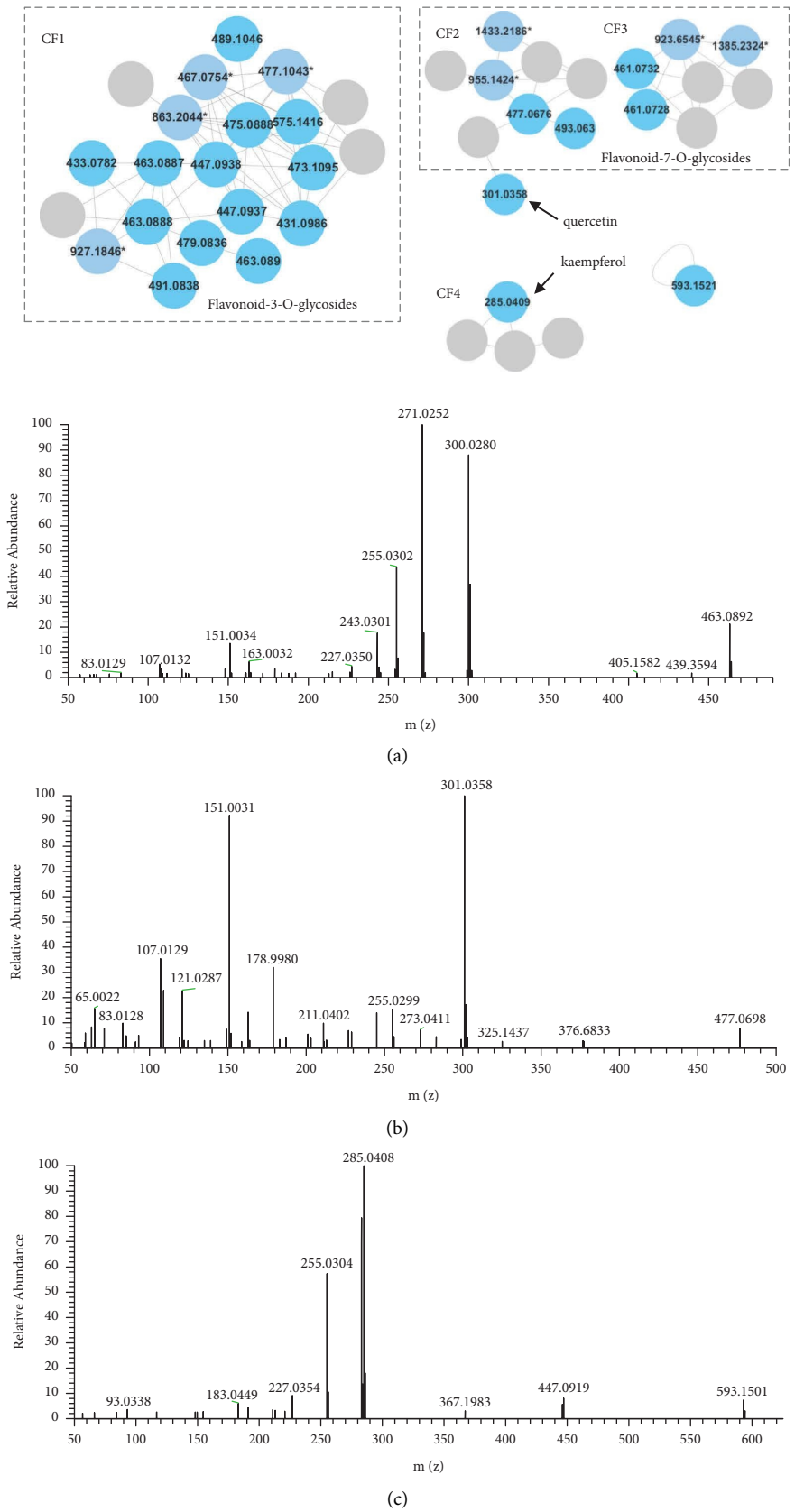

FIGURE 5: Molecular network of flavonoids from LCP and MS^2 spectra of isoquercitrin (a), quercetin-7-O-glucuronide (b), and kaempferol-7-O-glucoside-O-rhamnoside (c). Flavonoid-3-O-glycosides were mainly included in cluster CF1, while flavonoid-7-O-glycosides were clustered in CF2 and CF3. The nodes filled with bright blue and grey blue represent $[M-H]^-$ and adduct ions of compounds, respectively. The chemical structure nodes filled with grey colour are not annotated in present work.

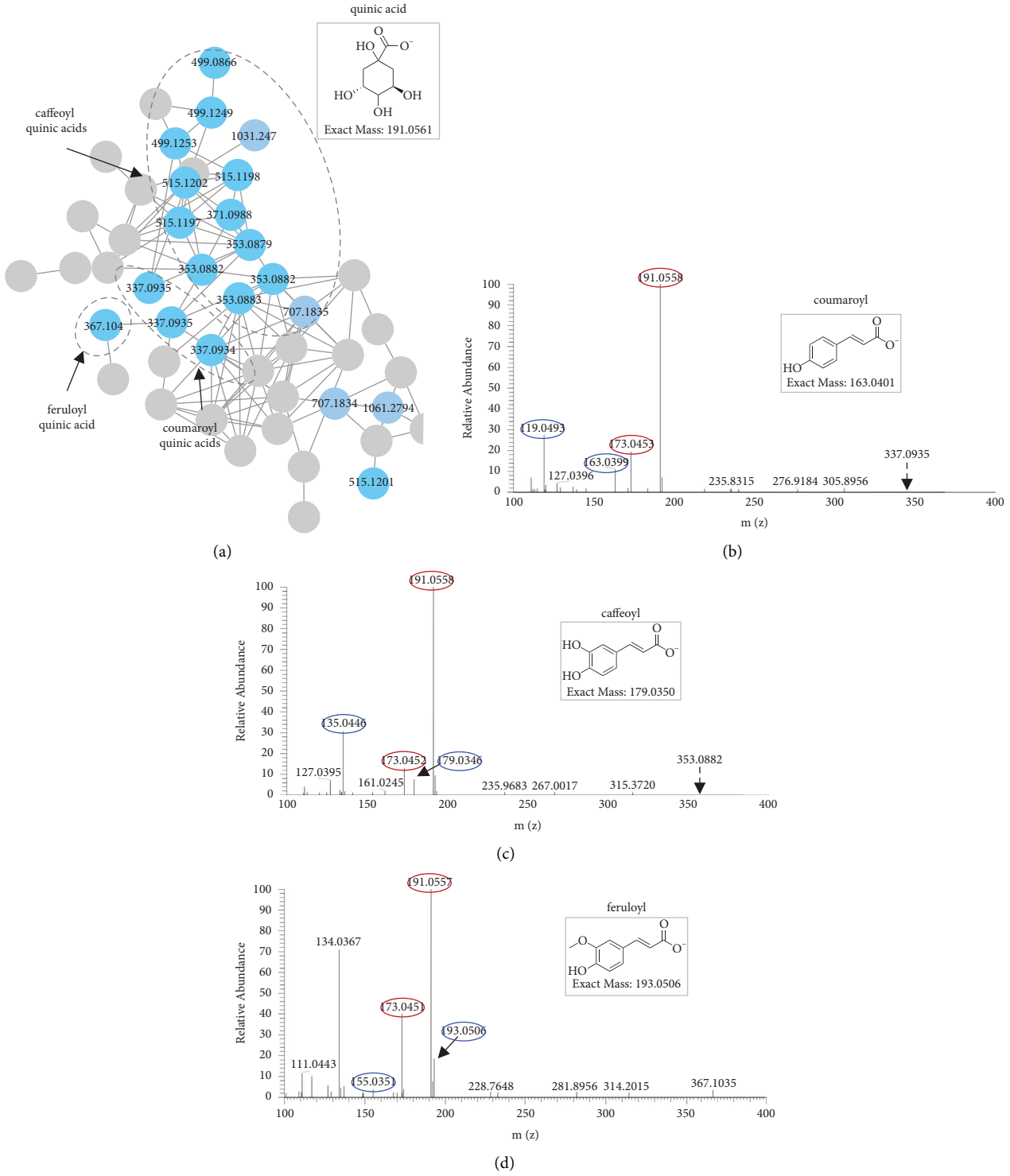

FIGURE 6: Molecular networking of quinic acid derivatives (a) and MS/MS spectra of coumaroyl quinic acid (b), chlorogenic acid (c), and 3-O-feruloylquinic acid (d) in LCP. The nodes filled with bright blue and grey blue represent $[M-H]^-$ and adduct ions of compounds, respectively. The chemical structure nodes filled with grey colour are not annotated in present work.

MolNetEnhancer. In these quinic acid derivatives, diagnostic ions of m/z 163.0397, 179.0347, and/or 193.0504 were determined, indicating the presence of coumaroyl, caffeoyl, and feruloyl units in quinic acid derivatives from LCP. The typical loss of CO_2 $[M-H-44]^-$ was also observed for all hydroxycinnamic acids. For feruloyl units, the loss of a methyl group $[M-H-15]^-$ was detected [47]. In addition, the differences in the intensities of the characteristic fragment ions of quinic acid could be used to determine the substitution position of hydroxycinnamic acids in the quinic

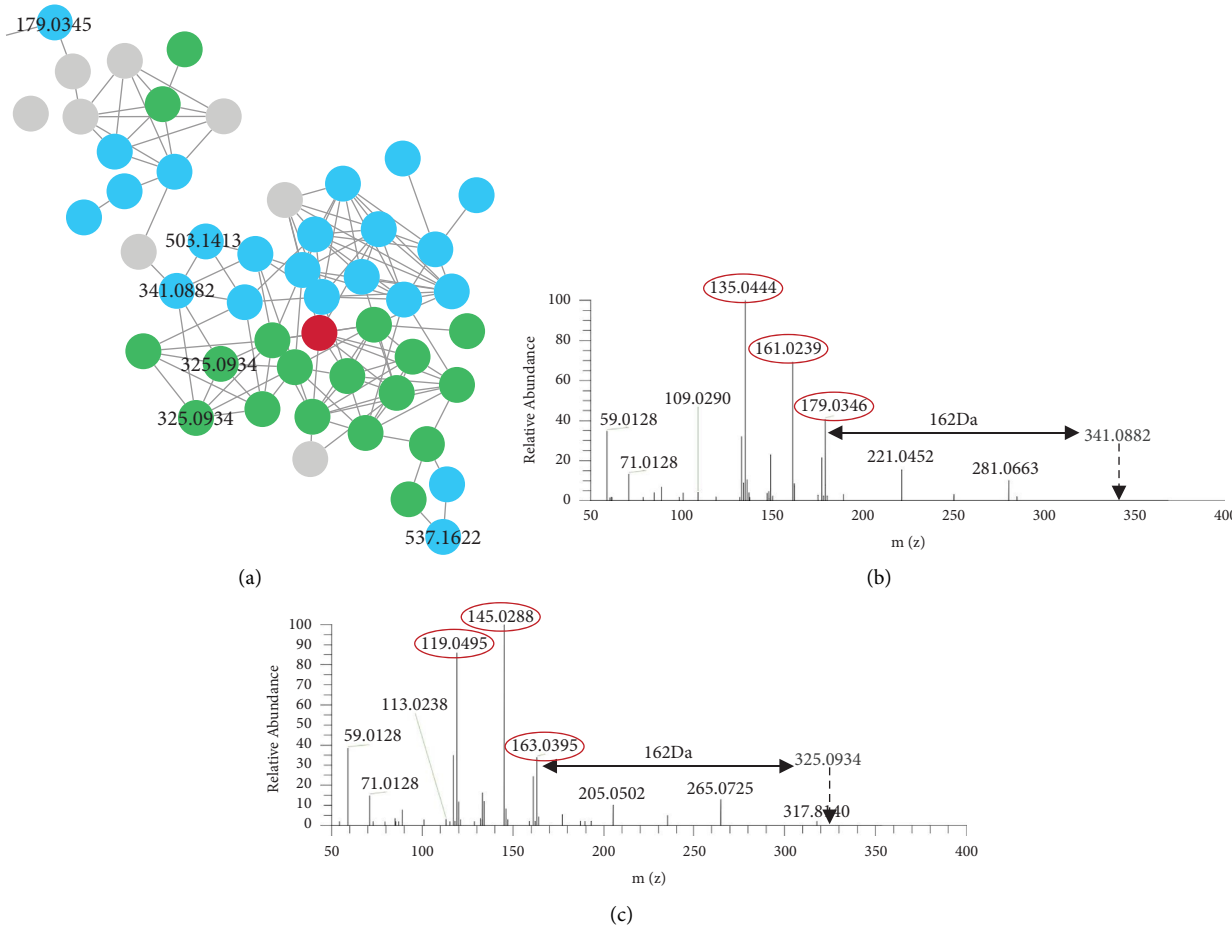

FIGURE 7: Molecular networking of phenolic compounds in LCP. The nodes with green, blue and red colour represent the compounds of coumaroyl derivatives, caffeoyl derivatives, and coumaroyl-caffeoyl derivatives, respectively (a). MS/MS spectra of caffeoyl glucoside (b) and coumaroyl glucoside (c).

acids [48]. According to the characteristic fragment ions listed in Table S1, 20 nodes in Figure 6 related to 16 quinic acid derivatives were identified.

In our study, characteristic fragment ions of coumaroyl and/or caffeoyl units were also detected in the MS/MS profiles of other compounds from LCP. Most of these compounds were included in the cluster as shown in Figure 7(a). Compounds 3 and 7, which had $[M-H]^-$ precursor ions at m/z 341.0882 and 325.0934, respectively, were inferred to contain coumaroyl and caffeoyl units because of the main fragment ions at m/z 179.03 [caffeoyl-H]$^-$, 161.02 [caffeoyl-H-H_2O]$^-$, 135.04 [caffeoyl-H-CO_2]$^-$, 163.04 [coumaroyl-H]$^-$, 145.03 [coumaroyl-H-H_2O]$^-$, and 119.05 [coumaroyl-H-CO_2]$^-$. A neutral loss of 162 Da was observed in the MS/MS profiles of compounds 3 and 7, indicating the presence of a glucoside moiety. Therefore, compounds 3 and 7 were tentatively identified as caffeoyl glucoside and coumaroyl glucoside, respectively. In addition, compound 19 was annotated as (1S, 4aS, 7S, 7aS)-1-[(2S, 3R, 4S, 5S, 6R)-6-[[(E)-3-(3,4-dihydroxyphenyl)prop-2-enoyl]oxymethyl]-3,4,5-trihydroxyoxan-2-yl]oxy-7-hydroxy-7-methyl-4a,5,6,7a-tetrahydro-1H-cyclopenta[c]pyran-4-carboxylic acid by the GNPS database. From the structure shown in Figure S1, the unit of caffeoyl glucoside in the compounds can be easily observed.

4. Conclusions

Components with antioxidant activity are the major active compounds in LCP. In the present work, the UAE of antioxidants from LCP was determined by single-factor analysis and RSM. With the optimal extraction conditions, the antioxidant yields reached 516.20 ± 28.52 μmol TE/ml. In addition, UHPLC-Q-Exactive Orbitrap-MS-based MN was applied to identify the active ingredients in the antioxidants. In all, 42 compounds with antioxidant activity in LCP were definitively or tentatively characterised, including 20 flavonoids, 16 quinic acid derivatives, 4 caffeoyl derivatives, and 2 coumaroyl derivatives.

The findings of the present work indicate that LCP leaves could be a good source of natural antioxidant compounds and, hence, could be applicable in the development of potential pharmaceutical drugs targeting diseases related to oxidative stress. Nevertheless, further studies using animal models are required to isolate active compounds, identify which ingredients are the main

antioxidant compounds, and clarify their antioxidant mechanisms.

Data Availability

The data used to support the findings of this study are included within the article.

Conflicts of Interest

The authors declare that there are no conflicts of interest.

Authors' Contributions

All authors contributed to the study conception and design. Yingpeng Tong, Junmin Li, and Jianxin Wang conceptualized the study; Yingpeng Tong and Xin Li handled methodology; Yingpeng Tong was in charge of original draft preparation; Ziping Zhu, Ting Wang, and Qi Zhou were in charge of writing reviews and editing; Na Li, Zhenda Xie, and Chunxiao Jiang handled visualization; Junmin Li and Jianxin Wang were in charge of supervision. All authors have read and agreed to the published version of the manuscript.

Acknowledgments

This research was funded by the Zhejiang Provincial Key Research and Development Program under grant no. 2018C02021.

Supplementary Materials

Table S1: peak assignments for ingredients in the antioxidant extraction of LCP. Figure S1: the structure of (1S, 4aS, 7S, 7aS)-1-[(2S, 3R, 4S, 5S, 6R)-6-[[(E)-3-(3,4-dihydroxyphenyl)prop-2-enoyl]oxymethyl]-3,4,5-trihydroxyoxan-2-yl]oxy-7-hydroxy-7-methyl-4a,5,6,7a-tetrahydro-1H-cyclopenta[c]pyran-4-carboxylic acid. The unit of caffeoyl glucoside in compounds are marked in red. (*Supplementary Materials*)

References

[1] X. Lei, W.-B. Hu, Z.-W. Yang et al., "Enzymolysis-ultrasonic assisted extraction of flavanoid from *Cyclocarya paliurus* (Batal) Iljinskaja:HPLC profile, antimicrobial and antioxidant activity," *Industrial Crops and Products*, vol. 130, pp. 615–626, 2019.

[2] W. Liu, S. Deng, D. Zhou et al., "3, 4-seco-Dammarane triterpenoid saponins with anti-inflammatory activity isolated from the leaves of *Cyclocarya paliurus*," *Journal of Agricultural and Food Chemistry*, vol. 68, no. 7, pp. 2041–2053, 2020.

[3] J.-H. Xie, F. Zhang, Z.-J. Wang, M.-Y. Shen, S.-P. Nie, and M.-Y. Xie, "Preparation, characterization and antioxidant activities of acetylated polysaccharides from *Cyclocarya paliurus* leaves," *Carbohydrate Polymers*, vol. 133, pp. 596–604, 2015.

[4] W. Yang, C. Jiang, Z. Wang et al., "*Cyclocarya paliurusextract* attenuates hepatic lipid deposition in HepG2 cells by the lipophagy pathway," *Pharmaceutical Biology*, vol. 58, no. 1, pp. 838–844, 2020.

[5] X. Zheng, M.-G. Zhao, C.-H. Jiang et al., "Triterpenic acids-enriched fraction from *Cyclocarya paliurus* attenuates insulin resistance and hepatic steatosis via PI3K/Akt/GSK3 beta pathway," *Phytomedicine*, vol. 66, Article ID 153130, 2020.

[6] W. Yan, L. Jiang, and J. Xu, "*Cyclocarya paliurus* (Batal.) Iljinskaja polysaccharides alleviate type 2 diabetes mellitus in rats by resisting inflammatory response and oxidative stress," *Food Science and Technology*, vol. 40, no. 1, pp. 158–162, 2020.

[7] B. P. Kilari, P. Mudgil, S. Azimullah, N. Bansal, S. Ojha, and S. Maqsood, "Effect of camel milk protein hydrolysates against hyperglycemia, hyperlipidemia, and associated oxidative stress in streptozotocin (STZ)-induced diabetic rats," *Journal of Dairy Science*, vol. 104, no. 2, pp. 1304–1317, 2021.

[8] A. P. Delli Bovi, F. Marciano, C. Mandato, M. A. Siano, M. Savoia, and P. Vajro, "Oxidative stress in non-alcoholic fatty liver disease. An updated mini review," *Frontiers of Medicine*, vol. 8, Article ID 595371, 2021.

[9] P. Zhang, T. Li, X. Wu, E. C. Nice, C. Huang, and Y. Zhang, "Oxidative stress and diabetes: antioxidative strategies," *Frontiers of Medicine*, vol. 14, no. 5, pp. 583–600, 2020.

[10] O. Sekiou, M. Boumendjel, F. Taibi, A. Boumendjel, and M. Messarah, "Mitigating effects of antioxidant properties of Artemisia herba alba aqueous extract on hyperlipidemia and oxidative damage in alloxan-induced diabetic rats," *Archives of Physiology and Biochemistry*, vol. 125, no. 2, pp. 163–173, 2019.

[11] D. Karanovic, N. Mihailovic-Stanojevic, Z. Miloradovic et al., "Olive leaf extract attenuates adriamycin-induced focal segmental glomerulosclerosis in spontaneously hypertensive rats via suppression of oxidative stress, hyperlipidemia, and fibrosis," *Phytotherapy Research*, vol. 35, no. 3, pp. 1534–1545, 2021.

[12] A. Mosca, A. Crudele, A. Smeriglio et al., "Antioxidant activity of Hydroxytyrosol and Vitamin E reduces systemic inflammation in children with paediatric NAFLD," *Digestive and Liver Disease*, vol. 53, no. 9, pp. 1154–1158, 2021.

[13] Y. Ruan, J. Zheng, Y. Ren, J. Tang, J. Li, and D. Li, "Changes of urine metabolites in response to n-3 fatty acid supplements and their correlation with metabolic risk factors in patients with type 2 diabetes," *Food & Function*, vol. 10, no. 5, pp. 2471–2479, 2019.

[14] J.-H. Xie, M.-Y. Shen, M.-Y. Xie et al., "Ultrasonic-assisted extraction, antimicrobial and antioxidant activities of Cyclocarya paliurus (Batal.) Iljinskaja polysaccharides," *Carbohydrate Polymers*, vol. 89, no. 1, pp. 177–184, 2012.

[15] J. H. Xie, M. Y. Xie, S. P. Nie, M. Y. Shen, Y. X. Wang, and C. Li, "Isolation, chemical composition and antioxidant activities of a water-soluble polysaccharide from *Cyclocarya paliurus* (Batal.) Iljinskaja," *Food Chemistry*, vol. 119, no. 4, pp. 1626–1632, 2010.

[16] Y. Liu, S. Fang, M. Zhou, X. Shang, W. Yang, and X. Fu, "Geographic variation in water-soluble polysaccharide content and antioxidant activities of *Cyclocarya paliurus* leaves," *Industrial Crops and Products*, vol. 121, pp. 180–186, 2018.

[17] G.-L. Chen, M.-X. Fan, J.-L. Wu, N. Li, and M.-Q. Guo, "Antioxidant and anti-inflammatory properties of flavonoids from *lotus plumule*," *Food Chemistry*, vol. 277, pp. 706–712, 2019.

[18] J.-H. Xie, C.-j. Dong, S.-P. Nie et al., "Extraction, chemical composition and antioxidant activity of flavonoids from *Cyclocarya paliurus* (Batal.) Iljinskaja leaves," *Food Chemistry*, vol. 186, pp. 97–105, 2015.

[19] X. Shang, J.-N. Tan, Y. Du, X. Liu, and Z. Zhang, "Environmentally-friendly extraction of flavonoids from

Cyclocarya paliurus (batal.) Iljinskaja leaves with deep eutectic solvents and evaluation of their antioxidant activities," *Molecules*, vol. 23, no. 9, p. 2110, 2018.

[20] D. He, X. Peng, Y.-F. Xing et al., "Increased stability and intracellular antioxidant activity of chlorogenic acid depend on its molecular interaction with wheat gluten hydrolysate," *Food Chemistry*, vol. 325, Article ID 126873, 2020.

[21] P. Lin, Q. Wang, Y. Liu et al., "Characterization of chemical profile and quantification of representative components of DanLou tablet, a traditional Chinese medicine prescription, by UHPLC-Q/TOF-MS combined with UHPLC-TQ-MS," *Journal of Pharmaceutical and Biomedical Analysis*, vol. 180, Article ID 113070, 2020.

[22] Y. Cui, H. Yang, J. Jing et al., "Rapid characterization of chemical constituents of Gansuibanxia decoction by UHPLC-FT-ICR-MS analysis," *Journal of Pharmaceutical and Biomedical Analysis*, vol. 179, Article ID 113029, 2020.

[23] L.-M. Wang, P. Wang, T. Teka et al., "1H NMR and UHPLC/Q-Orbitrap-MS-Based metabolomics combined with 16S rRNA gut microbiota analysis revealed the potential regulation mechanism of nuciferine in hyperuricemia rats," *Journal of Agricultural and Food Chemistry*, vol. 68, no. 47, pp. 14059–14070, 2020.

[24] M. Wang, J. J. Carver, V. V. Phelan et al., "Sharing and community curation of mass spectrometry data with global natural products social molecular networking," *Nature Biotechnology*, vol. 34, no. 8, pp. 828–837, 2016.

[25] A. T. Aron, E. C. Gentry, K. L. McPhail et al., "Reproducible molecular networking of untargeted mass spectrometry data using GNPS," *Nature Protocols*, vol. 15, no. 6, pp. 1954–1991, 2020.

[26] H. Lei, Y. Zhang, J. Ye et al., "A comprehensive quality evaluation of Fuzi and its processed product through integration of UPLC-QTOF/MS combined MS/MS-based mass spectral molecular networking with multivariate statistical analysis and HPLC-MS/MS," *Journal of Ethnopharmacology*, vol. 266, Article ID 113455, 2021.

[27] H. Lei, Y. Zhang, X. Zu et al., "Comprehensive profiling of the chemical components and potential markers in raw and processed *Cistanche tubulosa* by combining ultra-high-performance liquid chromatography coupled with tandem mass spectrometry and MS/MS-based molecular networking," *Analytical and Bioanalytical Chemistry*, vol. 413, no. 1, pp. 129–139, 2021.

[28] J. Houriet, P.-M. Allard, E. F. Queiroz et al., "A mass spectrometry based metabolite profiling workflow for selecting abundant specific markers and their structurally related multi-component signatures in traditional Chinese medicine multi-herb formulae," *Frontiers in Pharmacology*, vol. 11, Article ID 578346, 2020.

[29] W. Wang, R.-F. Yue, Z. Jin et al., "Efficiency comparison of apigenin-7-O-glucoside and trolox in antioxidative stress and anti-inflammatory properties," *Journal of Pharmacy and Pharmacology*, vol. 72, no. 11, pp. 1645–1656, 2020.

[30] S. Shi, K. Guo, R. Tong, Y. Liu, C. Tong, and M. Peng, "Online extraction–HPLC–FRAP system for direct identification of antioxidants from solid Du-zhong brick tea," *Food Chemistry*, vol. 288, pp. 215–220, 2019.

[31] R. Gunes, I. Palabiyik, O. S. Toker, N. Konar, and S. Kurultay, "Incorporation of defatted apple seeds in chewing gum system and phloridzin dissolution kinetics," *Journal of Food Engineering*, vol. 255, pp. 9–14, 2019.

[32] L.-F. Nothias, D. Petras, R. Schmid et al., "Feature-based molecular networking in the GNPS analysis environment," *Nature Methods*, vol. 17, no. 9, pp. 905–908, 2020.

[33] M. Ernst, K. B. Kang, A. M. Caraballo-Rodríguez et al., "MolNetEnhancer: enhanced molecular networks by integrating metabolome mining and annotation tools," *Metabolites*, vol. 9, no. 7, p. 144, 2019.

[34] W. Tang, L. Lin, J. Xie et al., "Effect of ultrasonic treatment on the physicochemical properties and antioxidant activities of polysaccharide from *Cyclocarya paliurus*," *Carbohydrate Polymers*, vol. 151, pp. 305–312, 2016.

[35] J. Xiang, M. Zhang, F. B. Apea-Bah, and T. Beta, "Hydroxycinnamic acid amide (HCAA) derivatives, flavonoid C-glycosides, phenolic acids and antioxidant properties of *foxtail millet*," *Food Chemistry*, vol. 295, pp. 214–223, 2019.

[36] Y.-Q. Ma, X.-Q. Ye, Z.-X. Fang, J.-C. Chen, G.-H. Xu, and D.-H. Liu, "Phenolic compounds and antioxidant activity of extracts from ultrasonic treatment of satsuma Mandarin (*Citrus unshiu* marc.) peels," *Journal of Agricultural and Food Chemistry*, vol. 56, no. 14, pp. 5682–5690, 2008.

[37] M. Irakli, P. Chatzopoulou, and L. Ekateriniadou, "Optimization of ultrasound-assisted extraction of phenolic compounds: oleuropein, phenolic acids, phenolic alcohols and flavonoids from olive leaves and evaluation of its antioxidant activities," *Industrial Crops and Products*, vol. 124, pp. 382–388, 2018.

[38] E. Alipanahpour Dil, M. Ghaedi, A. Asfaram et al., "Magnetic dual-template molecularly imprinted polymer based on syringe-to-syringe magnetic solid-phase microextraction for selective enrichment of p-Coumaric acid and ferulic acid from pomegranate, grape, and orange samples," *Food Chemistry*, vol. 325, Article ID 126902, 2020.

[39] H. Lü, R.-P. Lee, J. Huang et al., "A new HPLC–UV method for the quantification of terpenoids and antioxidant activity of commercial loquat leaf tea and preparation," *Journal of Food Measurement and Characterization*, vol. 14, no. 2, pp. 1085–1091, 2020.

[40] S. Feng, Z. Luo, Y. Zhang, Z. Zhong, and B. Lu, "Phytochemical contents and antioxidant capacities of different parts of two sugarcane (*Saccharum officinarum* L.) cultivars," *Food Chemistry*, vol. 151, pp. 452–458, 2014.

[41] S.-x. Yang, B. Liu, M. Tang et al., "Extraction of flavonoids from *Cyclocarya paliurus* (Juglandaceae) leaves using ethanol/salt aqueous two-phase system coupled with ultrasonic," *Journal of Food Processing and Preservation*, vol. 44, no. 6, Article ID e14469, 2020.

[42] K. Ablajan and A. Tuoheti, "Fragmentation characteristics and isomeric differentiation of flavonol O-rhamnosides using negative ion electrospray ionization tandem mass spectrometry," *Rapid Communications in Mass Spectrometry*, vol. 27, no. 3, pp. 451–460, 2013.

[43] M. Feng, Z. Zhu, L. Zuo et al., "A strategy for rapid structural characterization of saponins and flavonoids from the testa of *Camellia oleifera* Abel seeds by ultra-high-pressure liquid chromatography combined with electrospray ionization linear ion trap-orbitrap mass spectrometry," *Analytical Methods*, vol. 7, no. 14, pp. 5942–5953, 2015.

[44] J. Zhang, Q. Shen, J. C. Lu et al., "Phenolic compounds from the leaves of *Cyclocarya paliurus* (Batal.) Ijinskaja and their inhibitory activity against PTP1B," *Food Chemistry*, vol. 119, no. 4, pp. 1491–1496, 2010.

[45] Y. Kiselova-Kaneva, B. Galunska, M. Nikolova, I. Dincheva, and I. Badjakov, "High resolution LC-MS/MS characterization of polyphenolic composition and evaluation of

antioxidant activity of *Sambucus ebulus* fruit tea traditionally used in Bulgaria as a functional food," *Food Chemistry*, vol. 367, Article ID 130759, 2022.

[46] M. N. Clifford, I. B. Jaganath, I. A. Ludwig, and A. Crozier, "Chlorogenic acids and the acyl-quinic acids: discovery, biosynthesis, bioavailability and bioactivity," *Natural Product Reports*, vol. 34, no. 12, pp. 1391–1421, 2017.

[47] M. De Rosso, S. Colomban, R. Flamini, and L. Navarini, "UHPLC-ESI-QqTOF-MS/MS characterization of minor chlorogenic acids in roasted Coffea arabica from different geographical origin," *Journal of Mass Spectrometry*, vol. 53, no. 9, pp. 763–771, 2018.

[48] H. Ouyang, J. Li, B. Wu et al., "A robust platform based on ultra-high performance liquid chromatography Quadrupole time of flight tandem mass spectrometry with a two-step data mining strategy in the investigation, classification, and identification of chlorogenic acids in *Ainsliaea fragrans* Champ," *Journal of Chromatography A*, vol. 1502, pp. 38–50, 2017.